IOSR Journal of Applied Physics (IOSR-JAP)
e-ISSN: 2278-4861.Volume 6, Issue 6 Ver. II (Nov.-Dec. 2014), PP 28-41
www.iosrjournals.org

The possibility of using a simple pulse mode parallel plate gas ionization chamber, without Frisch grid, both for energy estimation and Z-identification of moderate energy light heavy ions

Rathin Saha
Variable Energy Cyclotron Centre, Department of Atomic Energy, Govt. of India
1/AF, Bidhan Nagar, Kolkata 700 064, India

Abstract: *This work explores theoretically the possibility of using a simple pulse mode parallel plate gas ionization chamber, having no Frisch grid, both for energy estimation and Z-identification of moderate energy light heavy ions. A mathematical expression for the energy of a heavy ion that enters into the ionization chamber through the cathode window and gets stopped in the sensitive volume is derived. An expression for a quantity similar to the range of the heavy ion is also derived. The plot of energy against this quantity is expected to give an opportunity to use a simple pulse mode parallel plate gas ionization chamber, without Frisch grid, as a light heavy Z-identifier. This work is based on the measurement of the electron collection pulse height and two other heights that the electron collection pulse reaches at two pre-calculated instants of time during the pulse rise time. A 'preset pulse clipper', the basic principle of which was proposed in a previous paper, may be used to measure the heights. Measuring heights - without using the 'preset pulse clipper' - by means of digital sampling and software based processing techniques may be possible if it be possible to determine the start time of the digitized pulse. One possible method for determining the start time of the digitized pulse is evaluated. The simulated plots, which represent the expected identification capability of this method, are made considering all the phenomena relevantly associated from physical point of view.*

Keywords*: Pulse mode parallel plate gas ionization chamber, electron collection pulse, Z-identification of moderate energy light heavy ions, ionization tracks of heavy ions, the start time of a digitized pulse.*

I. Introduction

A pulse mode parallel plate gas ionization chamber (PMPPGIC) is operated only by way of collection of electrons in the interest of having fast time response. At the moment when all the electrons are just collected, the total charge on the anode is the algebraic sum of the charge of the electrons and the charge induced by the positive ions. Since the charge induced depends on the distances of the positive ions from the anode, the total charge on the anode for a given number of electrons may be different at different situation. And that results in the formation of different electron collection pulse heights for a given energy. So an electron collection pulse mode parallel plate ionization chamber is not suitable for energy measurement [1, 2].

In order to eliminate the effect of positive ions, the anode plate is shielded from the positive ions by introducing a grid, known as Frisch grid, between the parallel plates [2, 3]. Once the anode is shielded from the effect of the positive ions, the pulse height is determined by the collected electrons only. But, in the present work we have shown that the effect of positive ions may also be eliminated without the use of a Frisch grid. A simple PMPPGIC, having no Frisch grid, may be shown, theoretically, to be suitable for Z-identification and energy estimation of moderate energy light heavy ions. Because of low stopping power in gases this method is expected to be confined to moderate energy heavy ions. In other words we have tried to study theoretically the possibility of using a simple PMPPGIC - having no Frisch grid - for Z-identification and energy estimation of moderate energy light heavy ions. It may be necessary to mention explicitly that no second detector, in addition to the PMPPGIC, is required to be used in the proposed technique.

A mathematical expression for the energy of a heavy ion that enters the ionization chamber through the cathode window and gets stopped in the sensitive volume is derived. An expression of a quantity similar to the range of the heavy ion is also derived. The plot of energy against this quantity is expected to give an opportunity to use a simple PMPPGIC, without Frisch grid, as a heavy Z identifier. This theoretical work uses the concept of measuring the height that a preamplifier pulse reaches at a pre-calculated time during the pulse rise time introduced in [4]. When Z-identification is required, for each incident heavy ion two/three measurements are required to be performed, namely measuring the height that the preamplifier pulse reaches at the moment of complete collection of all the generated electrons and the heights that the preamplifier pulse reaches at two pre-calculated instants of time during the pulse rise time. The necessary information on the range of heavy ions and the nature of heavy ion trajectories has been extracted from SRIM calculations.

II. Energy of the heavy ion stopped in the ionization chamber

2.1. Assumptions

The theory which may enable one to use a simple PMPPGIC for 'estimating energy and Z-identification of heavy ions' is based on the following assumptions:

1) 'The pressure of the gas and the strength of the electric field' in the ionization chamber are of such values that
a) the electron mobility (μ_e) is about1000 times larger than the ion mobility (μ_i),
b) the possibility of ion-electron recombination is negligible,
c) the plasma erosion time is negligible and
d) the diffusion of electrons and positive ions during the electron collection period is negligibly small.
2) The gases in the ionization chamber are free from electronegative impurities which have large cross-sections for capturing electrons to form negative ions. So, electrons only are responsible to form the negative charges.
3) The gases in the ionization chamber are distributed homogeneously.
4) The heavy ion enters the sensitive volume of the ionization chamber through a very thin cathode window and loses its full energy in the sensitive region of the chamber mainly by creating electron-ion pairs. The probability that the heavy ion suffers range scattering in the gas is very much less and the ionization track remains almost straight in turn.
5) The created electrons and ions are distributed along the track of ionization in an identical pattern and symmetrically around the track of ionization. As a result the centroid of the electrons is in coincidence with that of the ions at the beginning.
6) The symmetrical nature and the distribution pattern of both electrons and ions remain unchanged as long as none of the electrons or ions has reached the electrodes.
7) The charge collection time constant is such that the collected pulse reflects only the electron drift.

(The assumptions at serial nos. 1), 2) & 7) are the conditions normally encountered in a pulse mode gas ionization chamber.)

2.2 Derivation of the expression of energy

Let us consider a PMPPGIC whose anode surface is represented by x=0 plane and the cathode surface is represented by the x=w plane (Fig. 1). w is the distance of separation between the two parallel electrodes. The direction of electric field between the two electrodes is parallel to the x-axis. The magnitude of the same is given by

$$F=V/w \qquad (1)$$

where V is the bias voltage applied between the two electrodes.

The heavy ion enters the sensitive volume of the ionization chamber through a very thin cathode window and loses its full energy therein mainly by creating electron-ion pairs. And the track of ionization originated from the cathode window makes an angle with the electric field direction. Electrons and positive ions created along the ionization track of the heavy ion move in opposite directions under the influence of the electric field. The drift velocities of the electrons (v_e) and the positive ions (v_i) are given respectively by

$$v_e = \mu_e \frac{F}{p} \text{ and } v_i = \mu_i \frac{F}{p} \qquad (2)$$

where p is the gas pressure in the ionization chamber. At low values of F/p (which are normally encountered in a pulse mode gas ionization chamber) the order of magnitude of the electron mobility for most of the gases is 10^6(cm/s) $(V/cm)^{-1}$torr which is around 1000 times higher than that of the positive ion. As $\mu_e \approx 1000\mu_i$, the ions may be taken to be at rest during the electron collection period. In an ionization chamber, for which w=40cm, ions traverse a negligible distance of 0.4mm (approx) during the electron collection period. So, during the electron collection period the positive ions are effectively at rest. It is important to mention that the electron drift velocity in a pulse mode ionization chamber is normally maintained in the range from 5 to 6 cm/μs in the interest of having fast time response.

The electrons and ions created at x=w may be named first electrons and first ions respectively. Let R_c be the distance between the centroid of the first electrons (CFE) and the centroid of all the electrons (i.e., the centroid of the created electron cloud). Since most of the tracks of heavy ions are supposed to be straight (unlike the light ions), the angle of orientation of R_c may be taken to be equal to the angle of incidence. The centroid of the electrons is in coincidence with that of the ions at the beginning. R_c may be named mean distance of electrons or ions from the entrance window at the beginning. Let us assume that at time t=0 the centroid of the electrons just starts getting separated from that of the ions under the influence of the electric field. Since the pattern of the distribution of electrons remains unchanged, the value of R_c and its three dimensional orientation remains unchanged as long as none of the electrons has reached the anode.

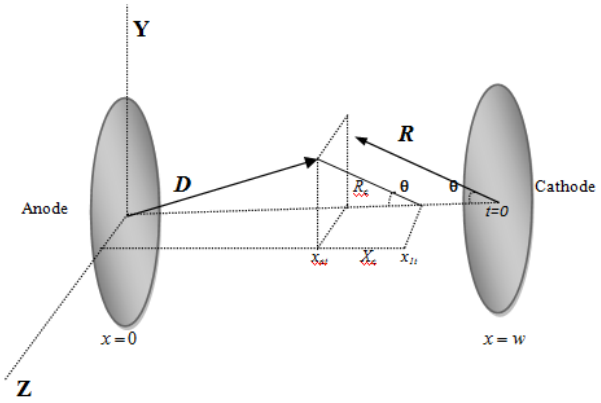

Fig. 1 Vector R represents the ionization track of the heavy ion at time t=0. x_{1t} and x_{ct} represent respectively the distance of the CFE from the anode surface and the distance of the centroid of all the electrons from the anode surface at time t. D is the position vector of the centroid of all the electrons at time t. R_c is the distance between the centroid of all the electrons and the CFE.

At time t (where $0 \leq t \leq w/v_e$) the position (Fig. 1) of the CFE is given by

$$x_{1t} = w - v_e t \quad (3)$$

In accordance with Ramo's Theorem [5] the expression of the charge induced Q_{te} on the anode by the electrons, as long as none of the electrons has reached the anode, can be written as

$$Q_{te} = q_e \sum_{n=1}^{N} \left(\frac{w - x_n}{w} \right) \quad (4)$$

where q_e is the electronic charge, N is the total number of electrons created, x_n is the distance of separation of the n^{th} electron from the anode when the distance of separation between the CFE and the anode is x_{1t}. $N = E/\varepsilon$, if E is the energy of the ionizing heavy ion and ε is the average energy required to form a free ion-electron pair.

The magnitude of the position vector ***D*** of the centroid of all the electrons is given by

$$|D| = \sqrt{\left(\frac{1}{N} \sum_{n=1}^{N} x_n \right)^2 + d^2} \,, \quad (5)$$

where d is the distance of the centroid of all the electrons from the x-axis. From Eqs.(4) and (5) one gets

$$Q_{te} = q_e N \left(1 - \sqrt{|D|^2 - d^2} \,/ w \right) = q_e N \left(1 - \frac{x_{ct}}{w} \right) \quad (6)$$

where x_{ct} is the distance of the centroid of all the electrons from the anode at time t. But $x_{ct} = x_{1t} - X_C$ where $X_C = R_C \cos\theta$ and θ is the angle of incidence. Now, in Eq. (6) Q_{te} can be written as the sum of two terms.

$$Q_{te} = q_e N \left(1 - \frac{x_{1t}}{w} \right) + q_e N \left(\frac{R_c \cos\theta}{w} \right) \quad (7)$$

Thus it appears that the expression of the charge induced by the electrons on the anode, as long as none of the electrons has reached the anode, consists of two terms the first one of which increases linearly with time whereas the rest one remains invariant with respect to time. The correctness of Eq. (7) from physical point of view can be understood once the charge, induced by the ions, is considered also simultaneously.

According to Eq. (3), $x_{1t} = w$ when t=0. So, at time t=0 the charge induced Q_{0e} by the electrons on the anode, found from Eq. (7), is given by

$$Q_{0e} = q_e N \left(\frac{R_c \cos\theta}{w} \right) \quad (7.1)$$

Since the displacement of the positive ions during the electron collection period is negligible, the charge induced Q_{ti} by the positive ions on the anode at any time t (where $0 \leq t \leq w/v_e$) can be found by replacing x_{1t} and q_e by w and q_i (ionic charge) respectively in Eq. (7) and the same is given by

$$Q_{ti} = q_i N\left(\frac{R_C \cos\theta}{w}\right) \qquad (7.2)$$

The total charge induced at time t (where value of t is such that none of the electrons has reached the anode) by the electrons and the ions, found by adding Eq. (7) to Eq.(7.2), is given by

$$Q_{ti} + Q_{te} = -eN\left(1-\frac{x_{1t}}{w}\right) = -e\frac{E}{\varepsilon}\left(1-\frac{x_{1t}}{w}\right)$$

where e represents the electronic charge. Then the height that the pulse reaches at time t is given by

$$H_t = \frac{Q_{ti}+Q_{te}}{C_f} = -c_0 E\left(1-\frac{x_{1t}}{w}\right) \qquad (7.3)$$

where $\mathbf{c}_0 = e/C_f\,\varepsilon$ and $\mathbf{C}_f$ is the feedback capacitor of the charge sensitive preamplifier compatible to the ionization chamber. Since only the amplitude of the pulse is the matter of interest, the negative sign is of no importance and E can be expressed as

$$E = \frac{H_t}{c_0\left(1-\frac{x_{1t}}{w}\right)} = \frac{E_t}{\left(1-\frac{x_{1t}}{w}\right)}, \text{ where } E_t = \frac{H_t}{c_0} \qquad (8)$$

Eq. (8) states that, as long as none of the electrons has reached the anode, the shape of the signal depends only on the number of electrons produced, i.e. the energy of the incident heavy ion. Another important outcome to be noted is that the value of E does not depend on the angle of incidence. Thus it may be possible to estimate the energy of the heavy ion by measuring the height that the preamplifier pulse reaches at a pre-calculated time during the pulse rise time, provided that none of the electrons has reached the anode within the pre-calculated time.

The condition under which Eq. (8) holds good implies that the value of x_{1t} should be greater than **R,** the range of the incident heavy ion. The larger the value of **R** the larger will be the required value of x_{1t}. But, E_t decreases with the increase of x_{1t} in accordance with Eq. (8). The measurement of E_t with good accuracy may not be possible if its value is very low. So, the value of x_{1t} is to be chosen suitably.

2.3. Elimination of the pulses generated from the heavy ions of range greater than x_{1t}

Every incident heavy ion, irrespective of its range, is supposed to yield a value of E_t. But, only such values of E_t as correspond to the heavy ions of range less than $\mathbf{x_{1t}}$ are acceptable. So the detector system is to be organized in such a way that all such values of E_t as correspond to the ranges that are greater than $\mathbf{x_{1t}}$ get rejected automatically.

Let E_{t_1} be the height which the preamplifier pulse reaches at time t_1, where $t_1<t$, during the pulse rise time. From Eq. (8) it is found that the ratio

$$E_t / E_{t_1} = (w - x_{1t}) / (w - x_{1t_1}) \qquad (9)$$

is a function of x_{1t} and x_{1t_1} only for a given **w**. Thus it is found that the ratio of E_t and E_{t_1} is independent of energy as long as the range is less than x_{1t} . If x_{1t} = 0.7 w and $x_{1t_1} = 0.75w$, the ratio E_t/E_{t_1} will be 1.2. A pulse, for which the ratio of E_t and E_{t_1} is not the same as the value yielded by Eq. (9), may be taken to have originated from a heavy ion of range greater than x_{1t} . So, the pulses for which Eq. (9) is not satisfied are to be eliminated.

2.4. Variation in the ratio E_t/E_{t_1}

Each electron collection pulse from the PMPPGIC is contaminated by unavoidable random electronic noise (Gaussian in nature) generated by the PMPPGIC itself, the preamplifier and other modules. So, in signals, which are identical in all respects, there will be a distribution in each of the values of E_t and E_{t_1} . Therefore, a distribution will also be associated with the ratio E_t/E_{t_1} . The expression of the standard deviation associated with the estimation of the ratio E_t/E_{t_1} (which is represented by r) is given by

$$\sigma_r = \left\{r\sqrt{1+r^2}/2.35(1-x_{1t}/w)\right\}(FWHM/E)\,, \qquad (10)$$

Where FWHM in keV represents the spread caused by 'electronic noise'. Table 1 gives the range of the predicted values of r under different experimental parameters. And $P_{(r\pm s\sigma_r)}$ represents the 'Gaussian Distribution predicted' probability that an experimental value of r will be confined to the range r ± S σ_r. In a given experimental condition a pulse for which r is not confined to the predicted range is to be rejected.

Table 1 The probable values of $r=E_t / E_{t1}$

r	E MeV	FWHM keV	σr	S	r± S σ_r	(Sσr/r) ×100	P(r± S σ_r)
1.2	20	30	0.0039	1	1.196 – 1.204	0.332	68.3
				1.64	1.1935 – 1.2065	0.545	90
				2.58	1.1897 – 1.2103	0.857	99
		20	0.0026	1	1.1973 – 1.2027	0.222	68.3
				1.64	1.1956 – 1.2044	0.363	90
				2.58	1.1931 – 1.2069	0.572	99
	100	30	0.00079	1	1.1992 – 1.2008	0.066	68.3
				1.64	1.1987 – 1.2013	0.109	90
				2.58	1.1979 – 1.2021	0.171	99
		20	0.00053	1	1.1995 – 1.2005	0.044	68.3
				1.64	1.1991 –1.2009	0.073	90
				2.58	1.1986 – 1.2014	0.114	99
	300	30	0.00026	1	1.1997 – 1.2003	0.022	68.3
				1.64	1.1996 – 1.2004	0.036	90
				2.58	1.1993 – 1.2007	0.057	99
		20	0.00017	1	1.1998 – 1.2002	0.015	68.3
				1.64	1.1997– 1.2003	0.024	90
				2.58	1.1995 – 1.2005	0.038	99

σ_r is calculated taking w=400mm, x_{1t}=0.7w and x_{1t1}=0.75w. The chosen values of s are encountered normally in estimating errors.

III. Identification of heavy ions

During the electron collection period $t_a = w/v_e$ the created electrons will be getting collected at the anode. So the total electronic charge accumulated on the anode at the end of the electron collection period will be q_eN. Since the displacement of the positive ions during the electron collection period is negligible, the charge Q_{t_ai} induced by the positive ions on the anode at time t_a will be the same as that given by Eq. (7.2). So the total charge on the anode at time t_a will be given by

$Q_{t_ae} + Q_{t_ai} = q_eN + q_iN\left(\frac{R_C\cos\theta}{w}\right) = -e\frac{E}{\varepsilon}\left(1-\frac{R_C\cos\theta}{w}\right)$ and the corresponding pulse height is given by $H_{t_a} = -c_0E\left(1-\frac{R_C\cos\theta}{w}\right)$. So the amplitude of the pulse at time t_a will be

$$H_{t_a} = c_0E\left(1-\frac{R_C\cos\theta}{w}\right) \text{ or } E_{t_a} = E\left(1-\frac{R_c\cos\theta}{w}\right) \quad (11)$$

If the angle of incidence be zero, the expression for the electron collection pulse height will be given by

$$H_{t_a} = c_0E\left(1-\frac{R_C}{w}\right) \text{ or } E_{t_a} = E\left(1-\frac{R_C}{w}\right), \text{ where } E_{t_a} = H_{t_a}/c_0 . \quad (11.1)$$

Eq. (11.1) states that the integrated signal depends on the mean position of the electrons (or ions) generated along the track of ionization and the energy of the heavy ion when the angle of incidence is zero.

The value of R_C obviously depends on the pattern of the distribution of the generated ion-electron pairs along the track of ionization. The Bethe-Bloch formula for non-relativistic heavy ions yields that for a given initial energy such distribution pattern depends on the identity of the heavy ion. So the value of R_C represents the identity of a heavy ion at a given energy. Thus, for a given energy, the value of R_C will be different for different type of heavy ions. The expression for R_C, found from Eqs. (8) and (11), is given by

$$R_C = \frac{w}{\cos\theta}\left\{1-\frac{E_{t_a}}{E_t}\left(1-\frac{x_{1t}}{w}\right)\right\} \quad (12)$$

Thus by measuring E_t and E_{t_a} it may be possible to plot E versus R_C for a given incident angle. Different curve, in the E versus R_C diagram for a given angle, is supposed to represent different type of heavy

ions. Thus the identification of heavy ions with the help of a simple PMPPGIC, based on electron collection, is expected to be possible. In the experiment one has to measure E_t and E_{ta} for each pulse and plot E versus R_C cosθ for identification purpose.

It can be shown relevantly that starting with an empirical range-energy relation of type $R = aE^b$ one can derive the basic formulas given by Eqs. (8) and (11.1). For this type of empirical relation one finds that $R_C = (b/(1+b))\,R$. Since the relation between R_c and R is linear, the plot of E versus R_c may be a substitute for the plot of E versus R.

IV. The possible techniques of measuring E_t and E_{t_1}

4.1 Using a proposed module named preset pulse clipper

For measuring the heights E_t and E_{t_1} a dedicated precision electronic module named preset pulse clipper, the basic principle of which has been proposed in [4], may be used. The preamplifier pulse is to be split into three identical pulses (preserving the original shape and height); one for measuring E_{t_a} (the electron collection pulse height) and the rest two for measuring E_t and E_{t_1}. The rest two are to be fed to two separate preset pulse clippers to get pulses corresponding to E_t and E_{t_1}. t and t_1 are the two delay times to be preset instrumentally in the two separate preset pulse clippers. It may be mentioned redundantly that the determination of t=0, the start time of the pulse, is not required here. The pulses corresponding to E_{t_a}, E_t and E_{t_1} can be processed by means of standard analog method followed for energy measurement. Then the evaluation of E and R_C will enable one to plot E versus R_C for heavy Z identification.

4.2 By means of digital sampling and software based processing techniques

It may be possible to measure the pulse heights E_t and E_{t_1} simply by means of digital sampling and software based processing techniques. A study of [6] may be helpful in this regard. The digitized signal E_{t_a} may be software managed to reproduce the basic principle of the proposed pulse clipper. The time slicing provided by a digitizer introduces a natural time scale whose each division is equal to the sampling period. So the pulse clipping times may be expressed in terms of sampling periods. Here, it is necessary to measure each signal always at the same precise times t and t_1 with respect to a reliable start time (i.e. we should have a reliable trigger which starts the digitization). From the physical point of view the start time is supposed to be approximately common for all the ions under identical experimental situation, but owing to the unavoidable electronic noise the start time will appear to have fluctuations. (To avoid any confusion it may be relevantly pronounced that the start time is not the time at which the ion enters the chamber. It is the time at which the centroid of the electrons just starts getting separated from that of the ions under the influence of the electric field, i.e. it is the point of time at which the pulse starts getting built up.). Now our aim is to determine the start time of the digitized pulse without which clipping a pulse is not possible.

4.2.1 Determination of the start time of the digitized pulse and maximum possible start time error

The height of the pulse at the start may be a clue for determining the start time. At the start the height of a given pulse should be zero. But, owing to the presence of electronic noise the height remains uncertain. So, it is necessary to choose justifiably a height - which may be named 'reference height' - very close to most of the possible heights at t=0. The value of the reference height should be so chosen that the start time can be proved to be confined to a well defined small span of time.

Now the height which 99% of the detector pulses, corresponding to a given energy **E**, will reach at time t during the pulse rise time is confined to the range

$$E_t = (Ev_e / w)t \pm 2.58\sigma_{RMS} \qquad \text{(a)}$$

where the 1st term comes from Eq.(8) and σ_{RMS} is the RMS electronic noise which is required to be determined before the start of the experiment. At t=0 the value of E_t will be confined to the range $\pm 2.58\sigma_{RMS}$ with 99% probability. When $t=t_{ref}$, where t_{ref} is given by

$$t_{ref} = 2 \times 2.58 w\sigma_{RMS} / (Ev_e) \qquad \text{(b)}$$

the value of E_t, which may be named $E_{t_{ref}}$, will be confined to the range from $2.58\sigma_{RMS}$ to $3\times 2.58\ \sigma_{RMS}$ with aforesaid probability. The lowest value of $E_{t_{ref}}$, which is $2.58\sigma_{RMS}$, may be taken as the required reference height for determining the start time of the pulse.

If the range of the heights at time t is given by Eq. (a), the condition, that two consecutive samples of the corresponding digitized pulse will invariably be of different values, can be written as

$$\tau > 2 \times 2.58 w \sigma_{RMS} / (E v_e) \qquad \text{(c)}$$

where τ is the sampling period of the digitizer. From (b) and (c) it is found that $\tau > t_{ref}$. If the value of E goes below a certain low value, the condition (c) will no more hold good, for a given value of τ.

When the reference height is equal to $2.58\sigma_{RMS}$ and $\tau > t_{ref}$, one may evaluate the start time in the following way:

The lowest digitized value of E_t - for which $(E_t - 2.58\sigma_{RMS}) > 0$ - may be taken to be the second sample of digitized pulse. Since this E_t, which may be named $E_{t_{(2nd)}}$, is the lowest but getter than $2.58\sigma_{RMS}$, the digitized value of $E_{t_{(2nd)-\tau}}$ (which is the digitized value of the sample just prior to the second sample) will obviously be either equal to or less than $2.58\sigma_{RMS}$, in accordance with the inequality (c). Hence the digitized value of $E_{t_{(2nd)-\tau}}$ may be approximated to be the first sample of the digitized pulse and the corresponding time may be taken as the start time, t=0, of the pulse with an error less than $\pm\tau$. This range of confinement of the error in determining the start time of the pulse can be understood if all of the relevant possible situations, written below, are examined keeping in mind that $\tau > t_{ref}$. The situations are:-

*if $t_{(2nd)}$ coincides with t_{ref}, it is obvious that $t_{(2nd)-\tau}$ <start time< $t_{(2nd)}$,

*if $t_{(2nd)}$ appears after t_{ref}, it is obvious that $t_{(2nd)-2\tau}$ <start time< $t_{(2nd)}$ and

*if $t_{(2nd)}$ appears before t_{ref}, it is obvious that $t_{(2nd)-\tau}$ <start time< $t_{(2nd)}$,

where $t_{(2nd)}$ is the instant of time at which the second sample of the digitized pulse occurs; similarly $t_{(2nd)-\tau}$ corresponds to the first sample and $t_{(2nd)-2\tau}$ corresponds to the sample prior to the first sample. And t_{ref} expresses the instant of time at which the period t_{ref} ends. Now, the software may be organized to find out the lowest valued sample for which $(E_t - 2.58\sigma_{RMS}) > 0$ and the same may be taken as the second sample of the digitized pulse; and the sample just prior to this will be taken as the first one.

If w=40 cm, FWHM of electronic noise=30keV, v_e= 5.5cm/μs, **S**=2.58 and the lowest energy of the incident heavy ions (E_{lowest}) =20MeV, the value of τ should be greater than 24ns as per the inequality (c). A digitizer of sampling period 25ns (i.e. a sampling frequency of 40 Msamples/s) may be used in this situation. Here the value of **S** is taken as 2.58 in view of that, for 99% of the pulses corresponding to a given energy, the start time can be determined with an error less than ±25ns. For a given set of w, v, **S** and E_{lowest} the lower the electronic noise the lower will be the required sampling period; again, the lower the sampling period the lower will be the error in determining the start time. Software based digital signal processing normally does not introduce any additional noise contribution. So the analog portion of the electronic chain is the only source of electronic noise. Therefore, the electronic noise generated by the analog portion of the electronic chain is one of the factors to decide the sampling period of the digitizer to be used. For 15keV electronic noise the value of τ may be around 15 ns.

The clipping time t, if expressed in terms of sampling periods, will appear as $t = n_i\tau + n_f\tau$, where n_i is an integer and n_f is a fraction. The pre-calculated value of the clipping time is to be adjusted to eliminate the fractional part $n_f\tau$. For a given pulse (corresponding to a given energy) the error, if exists, in determining the start time may appear as $+k_1\tau$ or $-k_2\tau$, where k_1 and k_2 are fractions (Fig. 2.1). In some situations k_2 only may exist. Fig. 2.2 shows a situation in which the start time error does not occur. Then the clipping time for a given pulse should ideally be written as $t = n_i\tau + k_1\tau$ or $t = n_i\tau - k_2\tau$ in general. Since the values of k's are not known, one may clip at $t = n_i\tau$ (with respect to the determined first sample of the digitized pulse) with an expected error of value either $+ k_1\tau$ or $- k_2\tau$ for a given energy. Thus the 'start time error' gets incorporated in the pulse clipping time.

The error in the clipping time causes an additional error in the value of E, besides the errors caused by electronic noise, the charge production statistics and such other factors as may be associated unavoidably. A little study of Fig. 2.1 yields that for a given energy $(k_1 + k_2) \leq 1$. When both the k's are nonzero the probability of occurrence of $+k_1\tau$ and $-k_2\tau$ may be taken to be equal because of the randomness of electronic noise. So the mean of the clipping time will be $t + \tau(k_1 - k_2)/2$ and the standard deviation associated with the clipping time will be $(k_1 + k_2)\tau/2$. Now, the expression of standard deviation σ_t (found using Eq. (8)) associated with E as a result of aforesaid uncertainty in the clipping time t, may reasonably be given by

$\sigma_t = (E/t)(k_1 + k_2)\tau/2$. Since, $(k_1 + k_2) \leq 1$ one may write $\sigma_t \leq (E/t)\tau/2$. To take only the account for maximum possible error arising out of the clipping time, one may write $\sigma_t = (E/t)\tau/2$. When w=40 cm, v_e=5.5cm/μs, $x_{1t} = 0.7w$, $x_{1t_1} = 0.75w$ and τ =25ns, one gets $t = 87\tau$ and $t_1 = 72\tau$ ignoring the fractional part $n_f\tau$ as discussed above**.** At 20, 100 and 300 MeV the estimated values of σ_t are 115, 575 and 1724keV respectively.

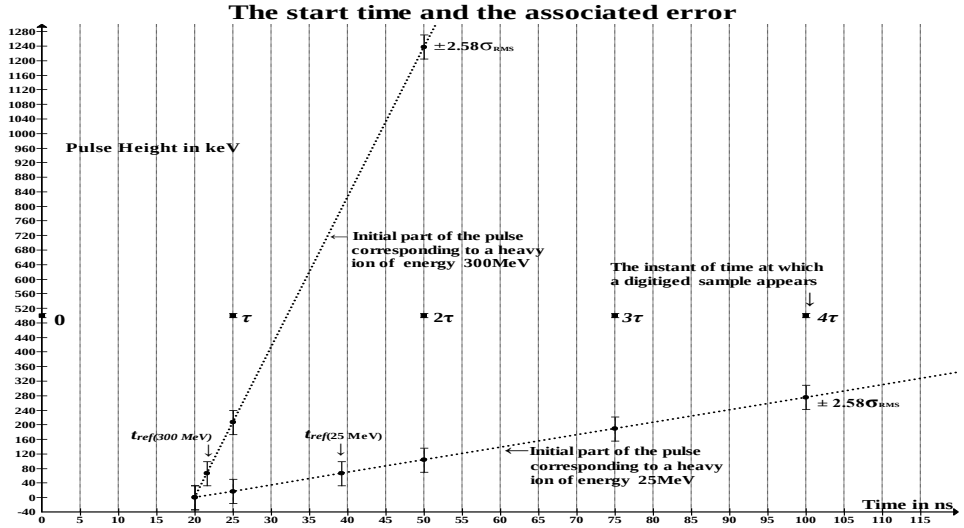

Fig. 2.1 It is assumed that each of the shown analog pulses start at 20 ns in reality and the samples of the corresponding digitized pulses appear at 0, τ, 2τ, 3τ, 4τ,…. where τ, the sampling period of the digitizer, is 25 ns. (a) For 25 MeV pulse: If the second sample appears at 25 ns, the sample at 0 ns may be taken to be the first sample of the pulse. So, the start time error in this situation will be −20 ns and may be expressed as $-k_2\tau$, where k_2=4/5. If the second sample appears at 50 ns, the sample at 25 ns may be taken to be the first sample with an error of +5 ns, or $+k_1\tau$, where k_1=1/5. Thus there may be two start times for a given energy. Since the amount of preset clipping time is the matter of interest and is kept fixed, the shifting of the start time will cause no problem in the experiment. (b) For 300 MeV pulse: It is obvious that the second sample will appear at 25 ns only. Because, 99% of the possible values of the sample at 25 ns (i.e. all the values of the sample within the error bars at 25 ns) will be higher than the defined reference height, which is $2.58\sigma_{RMS}$. So, the sample at 0 ns may be taken to be the first sample of the pulse with an error of − 20 ns or $-k_2\tau$, where k_2=4/5. (c) Thus this figure shows that the start time error is confined to the range $\pm\tau$ and $(k_1 + k_2) \leq 1$ in any of the situations in which a start time error occurs.

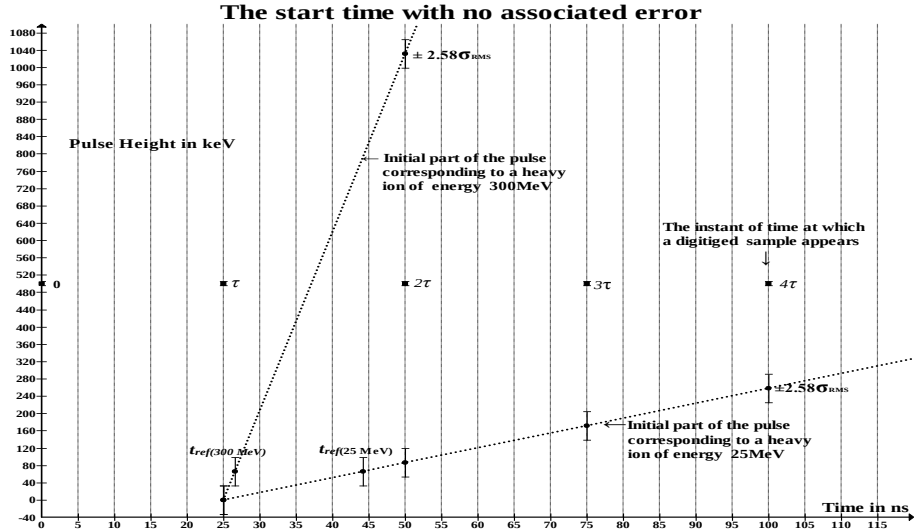

Fig. 2.2 It is assumed that in reality the start time of each of the shown analog pulses coincides with the instant of time (say 25 ns) at which a digitized sample appears and assumed also that the sampling period τ of the digitizer is 25 ns. For each of the two pulses it is obvious that the second sample will appear at 50 ns only. Because, 99% of the possible values of the sample at 50 ns (i.e. all the values of the sample within the error bars at 50 ns) will be higher

than the defined reference height, which is $2.58\sigma_{RMS}$. So the sample at 25 ns, which is just prior to the second sample, will be the first sample of each pulse. Thus this figure shows the possibility of occurrence of no start time error.

From the sets of three 'digitized and processed' pulses corresponding to E_{t_a} , E_t and E_{t_1} the software is organized to accept only those sets for each of which the ratio r is confined to a pre-estimated range r ± S σ_r (as discussed in Sub-section 2.4) i.e., the software has to do the job of accepting the pulses of all such heavy ions as are of range less than x_{1t}. Then the software may be further organized to calculate the values of E and R_C and plot E versus R_C for heavy Z identification.

V. Estimated results

5.1 Estimation of the values of E_t , E_{t_1} and E_{t_a}

If the sensitivity of the charge sensitive pre-amplifier be 1μV/electron-ion pair, the value of c_0 for P-10 gas may be taken to be 37.87mV/MeV. It is claimed (by SRIM itself) that the range of a heavy ion found by SRIM calculations is accurate, usually, within 5% of the actual experimental value. Assuming this claim of accuracy to be true one may estimate, from Eq. (11.1), the value of E_{t_a} taking R_C to be a fraction of the SRIM calculated range. In the calculation it has been assumed that R_C = 0.7R, where R represents the estimated range. It is assumed that the detector of interest is made of P-10 gas and its very thin entrance window of thickness 1μm is made of aluminized Paralene-C. Tables 2.1 and 2.2 give the estimations of E_t , E_{t_1} and E_{t_a} , for a number of moderate energy light heavy ions, made on the basis of the following assumed parameters: P=600 torr, T=300 ^{o}k, w=400mm, $x_{1t} = 0.7w$, $x_{1t_1} = 0.75w$ and θ=0°. The density of the P-10 gas at pressure 600 torr is $\rho_{P-10} \sim 1.115 mg/cm^3$. In Tables 2.1 and 2.2 each estimated R is less than x_{1t} . So Eq. (8) holds good for all the values of R appearing in Tables 2.1 and 2.2.

Table 2.1 Estimation of the values of H_t , H_{t_1} and H_{t_a}

w =400 mm, x_{1t} =0.7 w, x_{1t1} = 0.75 w, P = 600 torr, θ = 0° and ρ = 1.115mg/cm^3												
E	^{14}N		^{16}O		^{19}F		^{20}Ne		^{23}Na			
MeV	R mm	H_{t_a} mV	R mm	H_{t_a} mV	R mm	H_{t_a} mV	R mm	H_{t_a} mV	R mm	H_{t_a} mV	H_t mV	H_{t_1} mV
20	30.24	717	25.72	723	22.15	728	20.5	730	18.9	732	227	189
40	74.23	1318	60.06	1356	49.14	1384	42.5	1402	37.3	1416	454	387
60	131.25	1750	103.95	1859	82.21	1945	69.6	1995	60	2034	682	568
80	201.6	1961	155.4	2206	119.7	2395	100.9	2495	86.4	2572	909	757
90	241.5	1968	184.8	2306	140.7	2569	117.6	2707	100.7	2808	1022	851
100			215.25	2360	162.7	2709	135.4	2890	115.5	3022	1136	946
110			248.8	2352	185.8	2811	154.3	3041	131.2	3210	1245	1037
120					211	2866	175.3	3151	147	3376	1363	1135
130					237.3	2881	195.3	3241	164.8	3504	1477	1230
140					264.6	2847	217.3	3286	182.7	3607	1590	1325
150							241.5	3280	201.6	3677	1704	1420
160							264.6	3254	220.5	3721	1818	1515
170									241.5	3717	1931	1609
180									261.4	3699	2045	1704

Table 2.2 Estimation of the values of H_t, H_{t_1} and H_{t_a}

w =400 mm, x_{1t} =0.7 w, x_{1t1} = 0.75 w, P = 600 torr, θ = 0° and ρ = 1.115mg/cm^3												
E	^{24}Mg		^{27}Al		^{28}Si		^{31}P		^{32}S		H_t	H_{t_1}
MeV	R **mm**	H_{t_a} **mV**	R **mm**	H_{t_a} mV	R **mm**	H_{t_a} **mV**	R **mm**	H_{t_a} **mV**	R **mm**	H_{t_a} **mV**	**mV**	**mV**
20	**18.06**	**730**	**16.8**	**735**	**14.8**	**738**	**15**	**737**	**13.75**	**739**	**227**	**189**
40	**34.54**	**1416**	**30.87**	**1433**	**27**	**1443**	**26.35**	**1445**	**23.83**	**1452**	**454**	**387**
60	**54.6**	**2033**	**47.7**	**2082**	**41.8**	**2106**	**39.27**	**2116**	**35.38**	**2132**	**682**	**568**
80	**77.59**	**2572**	**66.7**	**2676**	**58.4**	**2720**	**53.55**	**2746**	**48.4**	**2773**	**909**	**757**
90	**90.3**	**2887**	**76.9**	**2950**	**67.4**	**3006**	**61.32**	**3043**	**55.33**	**3079**	**1022**	**851**
100	**103.42**	**3207**	**87.7**	**3205**	**76.7**	**3279**	**69.3**	**3328**	**62.47**	**3373**	**1136**	**946**
110	**116.55**	**3339**	**98.9**	**3445**	**86.6**	**3535**	**77.6**	**3600**	**69.93**	**3656**	**1245**	**1037**
120	**131.25**	**3376**	**110.2**	**3668**	**96.7**	**3776**	**86.2**	**3859**	**77.7**	**3927**	**1363**	**1135**
130	**145.95**	**3703**	**121.8**	**3874**	**107.1**	**4001**	**95**	**4105**	**85.68**	**4186**	**1477**	**1230**
140	**161.7**	**3607**	**134.4**	**4055**	**117.6**	**4211**	**104.3**	**4335**	**93.76**	**4433**	**1590**	**1325**
150	**177.45**	**3969**	**148**	**4210**	**129.1**	**4398**	**113.4**	**4554**	**102.2**	**4665**	**1704**	**1420**
160	**194.25**	**4056**	**160.6**	**4357**	**140.7**	**4568**	**122.8**	**4758**	**110.2**	**4891**	**1818**	**1515**
170	**212.1**	**4120**	**174.3**	**4475**	**152.2**	**4724**	**133.3**	**4937**	**119.7**	**5090**	**1931**	**1609**
180	**229.95**	**4162**	**189**	**4563**	**164.8**	**4851**	**144**	**5100**	**128**	**5290**	**2045**	**1704**
190	**248.85**	**4169**	**203.7**	**4631**	**177.4**	**4962**	**154**	**5257**	**137.5**	**5465**	**2159**	**1799**
200	**267.75**	**4138**	**218.4**	**4680**	**191.1**	**5042**	**164.8**	**5391**	**147**	**5627**	**2272**	**1893**
210	**287.7**	**4066**	**234**	**4697**	**204.7**	**5105**	**181.65**	**5624**	**157.5**	**5762**	**2386**	**1988**
220			**249.9**	**4688**	**218.4**	**5148**	**188**	**5591**	**168**	**5883**	**2500**	**2083**
230			**266.7**	**4645**	**232**	**5175**	**199.5**	**5670**	**178.5**	**5990**	**2613**	**2177**
240					**246.7**	**5166**	**212**	**5718**	**189**	**6084**	**2727**	**2272**
250					**262.5**	**5119**	**224.7**	**5746**	**199.5**	**6163**	**2840**	**2366**
260					**277.2**	**5070**	**237.3**	**5758**	**210**	**6229**	**2954**	**2461**
270							**250**	**5753**	**221.5**	**6263**	**3068**	**2556**
280							**263.5**	**5715**	**233**	**6281**	**3181**	**2651**
290							**277**	**5660**	**245.7**	**6256**	**3295**	**2746**
300									**257**	**6252**	**3409**	**2840**
310									**269.8**	**6194**	**3522**	**2935**

The range R of heavy ions is estimated from SRIM calculations. H_{ta}, H_t, and H_{t1} are calculated from Eqs. (8) and (11.1). H_{ta} is calculated assuming that R_c=0.7R.

5.2 E versus R_c plots for the identification of moderate energy light heavy Z

Now we consider the situation in which our proposed preset pulse clippers [4] have been used for clipping pulses. In Fig. 3 the thick lines represent expected E versus R_C (taking the data from Tables 2.1 and 2.2) plots for a number of different types of light heavy ions of moderate energy when the angle of incidence is zero. The dotted/thin lines in Fig. 3 represent the expected E versus 'projection of R_c' plots when the angle of incidence is 15°. When the angle of incidence is θ, the projection of R_c may be denoted by $R_c(\theta)$. In experiment $R_c(\theta)$ is to be calculated from Eq.(12) obtaining the experimental value of E_t and E_{t_a} .

$R_c(\theta)$ decreases with the increase of θ. Thus for a given type of heavy ions different dotted line for different angle of incidence is expected to appear. And, as θ increases, the separation between the thin and the dotted lines increases for a given type heavy ion.

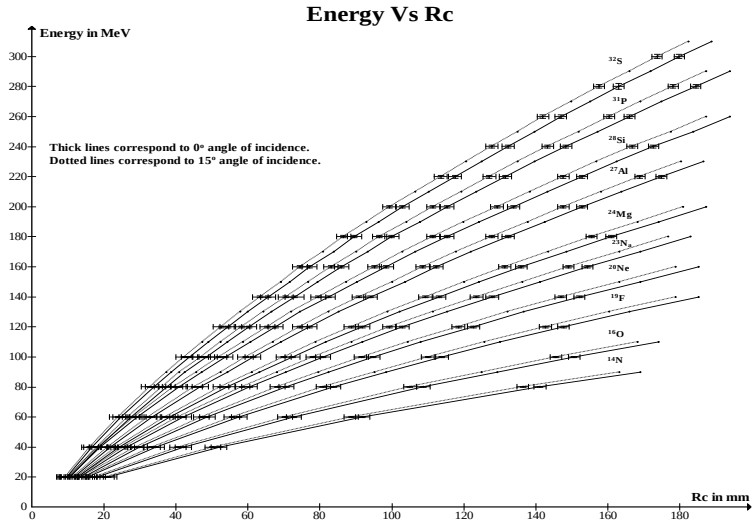

Fig. 3 The expected E versus R_c plots, for different types light heavy ions of moderate energy, are shown. Each pair of thick and thin lines represents a type of heavy ions. In an experiment, a dotted band will appear in place of each pair of lines.

It is natural that a normally incident ion beam must have an incident angular distribution. Because of this angular distribution one is supposed to get a dotted band instead of a line for each type of heavy ions in the E versus R_c diagram. Fig. 3 represents a situation in which the incident angular distribution is confined to the range from 0° to 15°. This angular distribution causes $R_c(\theta)$ to vary; for example, for ^{32}S ions of energy 300MeV, the values of the projected R_c varies from 173 to 179mm. Since in the present situation each band is well separated from the subsequent band, heavy ions of different Z-values can be distinguish. A study of the heavy ion trajectories, found by SRIM calculations, convinces us that for a normal incidence (i.e. when the incident angle of the beam is 0°) the incident angular distribution is almost confined to the range from 0° to 5°. So in a real experiment the separation between any two subsequent bands is expected to be good for the purpose of Z identification. Here it may be relevantly said our expectation is confined to the Z-identification only.

The estimated fluctuations, in the form of standard deviation, associated with the values of E and $R_c(\theta)$ are depicted in the plots. The total energy resolution of the ionization chamber may be written as:

$(FWHM)_{total} = \sqrt{(FWHM)^2_{stastical} + (FWHM)^2_{electronic} + (FWHM)^2_{other-sources}}$, where

* $(FWHM)_{statistical}$, the charge production statistical spread, derived from Eq. (8), is given by $(FWHM)_{stastical} = 2.35\sqrt{Ef\varepsilon/(1-x_{1t}/w)}$, f being the Fano factor.

* $(FWHM)_{electronic}$ is the spread caused by the noise generated by the analog portion - mainly by the preamplifier of the electronic chain - which may be taken to be 30keV typically.

* $(FWHM)_{other-sources}$ is the spread caused by other different sources like window thickness, unavoidable electric field distortion, ion motion, electron diffusion and other minor deviations from the conditions assumed in Sub-section 2.1.

The aforesaid spreads introduce fluctuations in the projected range which in turn introduce fluctuations in $R_c(\theta)$. The expression of fluctuations in $R_c(\theta)$, in the form of standard deviation, derived out of Eq. (12), is given by

$$\sigma_{R_c(\theta)} = \sqrt{\frac{2}{1-(1-x_{1t}/w)^2}}\,\frac{w}{E}\left(1-\frac{R_c\cos\theta}{w}\right)(\sigma_E)_{total} \qquad (13)$$

The following values may relevantly be assumed in estimating (FWHM) $_{\text{statistical}}$ and $\sigma_{R_C(\theta)}$: f=0.2 (a typical value for gas), $x_{1t} = 0.7w$, w=400mm, and $\varepsilon = 26.4eV$. At 20, 100 and 300 MeV the estimated values of (FWHM) $_{\text{statistical}}$ are 0.22%, 0.1% and 0.06% respectively. It may not be possible to estimate theoretically the values of (FWHM) $_{\text{other-sources}}$. However, it may be reasonable to assume (FWHM) $_{\text{total}}$ to be 1%; because for fission fragments and heavy ions typical energy resolution figures found in different gas detectors are about 1% [7, 8]. For ^{32}S ions the estimated values of $\sigma_{R_c(0^\circ)}$ at energies 20, 100 and 300 MeV are 2.46, 2.25 and 1.38 mm respectively.

Since the incident angular distribution and fluctuations in E and $R_C(\theta)$, caused by the factors said above, are not avoidable, there will be a dotted band in the E versus R_C diagram for each Z-value. It is relevant to mention further that the estimated variation of $R_C(\theta)$ for a given θ exhibits the phenomena of range straggling, which is defined as the fluctuation in track length for individual ions of the same initial energy.

Now we consider the situation in which we adopt the digital sampling and software based processing techniques in place of using the proposed preset pulse clipper. In this situation, if the maximum value of σ_t, as discussed in Sub-section 4.2.1, is taken into consideration, it may be reasonable to expect that $\sigma_{overall}$ which may be given by $\sigma_{overall} = \sqrt{\sigma_{total}^{\ 2} + \sigma_t^{\ 2}}$ will be less than 0.7% of the heavy ion energy when τ = 25 ns and will be less than 0.55% when τ = 15 ns.

5.3 Error in the estimated E caused by the movement of ions

Since $v_e \approx 1000\ v_i$, the movement of the ions during the electron collection period is ignored in deriving the expression of energy E, given by Eq. (8). But in reality in time t, given by Eq. (3), the ions traverse an extremely small distance $(w - x_{1t}) / 1000$ towards the cathode; and in the present case this distance is only 0.12 mm as w=400 mm and x_{1t}=0.7w. The ion movement, if taken into account, will change the expression of Q_{ti} , given by Eq. (7.2), to

$Q_{ti} = q_i(N - \nabla N)\left\{\dfrac{(R_c - \nabla R_c)\cos\theta}{w}\right\}$, where ∇N represents the numbers of ions which have reached the cathode in time t and ∇R_C represents the reduction in R_C of the ion cloud at time t because of the arrival of the ∇N ions at the cathode. The modified expression of Q_{ti} when added to the expression of Q_{te} , given by Eq. (7), one arrives at the following equation in place of the Eq. (8):

$$E_t = E\left(1 - \frac{x_{1t}}{w}\right) + E\left(\nabla R_c + \frac{\nabla E}{E} R_c - \frac{\nabla E}{E}\nabla R_c\right)\frac{\cos\theta}{w} \qquad (14)$$

The expression of ∇E may be given by $\nabla E = \dfrac{(w - x_{1t})}{1000\cos\theta}\left(\dfrac{dE}{dx}\right)_E$, where $\left(\dfrac{dE}{dx}\right)_E$ represents the specific energy loss at incident energy E. For ∇R_c one may reasonably expect that $\nabla R_c < \dfrac{w - x_{1t}}{1000\cos\theta}$. Here it may be reasonable to approximate that $\nabla R_c = \dfrac{0.7(w - x_{1t})}{1000\cos\theta}$ because it has been assumed that $R_c = 0.7R$. On substituting the expressions of ∇E and ∇R_c it is found that modified expression of E_t is practically independent of the angle of incidence. Because $\nabla E \nabla R_c \dfrac{\cos\theta}{w}$, the only term that depends on θ , is negligibly small in comparison with other terms. The variation of θ in the range from 0º to 45º causes E_t (which is not less than 1MeV) to vary in a very short range of span a few tens of eV only.

From Eq. (15) one finds that the error caused by the motion of ions is given by

$$E_{err(ion)} = \frac{E}{1000}\left[0.7 + \frac{R_c}{E}\left(\frac{dE}{dx}\right)_E - \frac{0.7(w - x_{1t})}{1000E\cos\theta}\left(\frac{dE}{dx}\right)_E\right] \qquad (15)$$

$E_{err(ion)}$ is to be subtracted from the value of E (yielded by Eq. (8), the working relation) to take the effect of ion movement into consideration. Fig. 4 gives the estimated percentage error versus E plots for all the different types of heavy ions that appear in Tables 2. The variation of the percentage error with E is confined to a very small range of span less than 0.1%. So, it is obvious that $E_{err(ion)}$ versus E plot for each type of heavy ions will be linear, which implies that $E_{err(ion)}$ is almost directly proportional to E. In a real experiment it may be possible to estimate the values ∇R_c with help of E versus R_c plots and SRIM calculations. The values of ∇E can be estimated with the help of SRIM calculations only.

Because of the movement of ions, the ratio E_t / E_{t1} (i.e., r) will increase by an order 10^{-4}. Such a small change will not prevent the values of r to remain confined to the ranges $r \pm S\,\sigma_r$ estimated in Table 1. So the effect of the movement of ions on the values of r may be taken to be nil.

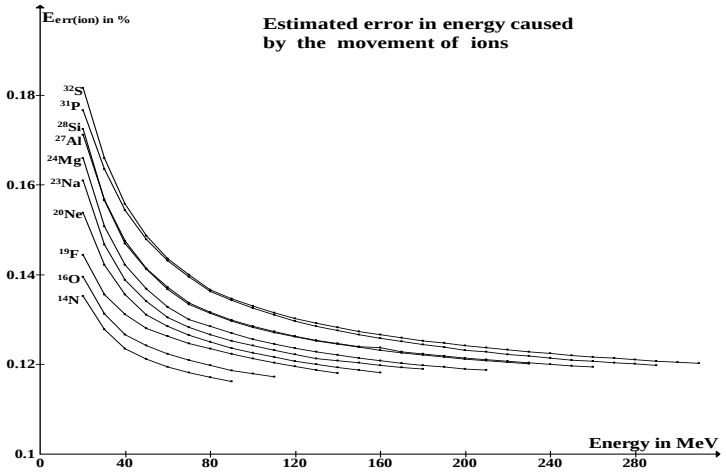

Fig. 4 Error, in the measurement of energy caused by the movement of positive ions, is plotted against the energy of the incident heavy ion. The values of $E_{err(ion)}$ are calculated choosing w=400 mm, x_{1t}=0.7w and R_c=0.7R.

5.4 Error in the estimated E caused by the diffusion of electrons

In deriving Eq. (8) it is assumed that the diffusion of electrons and positive ions is negligibly small. But in reality the effect of longitudinal electron diffusion cannot be neglected though it is very much small. In an ionization chamber, over a period of few microseconds that is typically required for the electrons to reach the anode, the diffusion of electrons in either direction (i.e., longitudinal or transverse to the electric field) might be of the order of one millimeter or less [9].

Since the created electrons are distributed symmetrically around the track of ionization, the transverse diffusion will cause an extremely thin symmetrical expansion of the electron cloud around the track of ionization. Since the expansion is symmetrical and transverse to the electric field, the magnitude of R_c of the electron cloud is not supposed to change. In addition to this, since it is a matter of transverse diffusion, the possibility of any additional longitudinal motion does not arise. So, it is expected that the transverse diffusion will not change the value of x_{1t}. But, owing to longitudinal diffusion the electron cloud as whole will get a minute motion, in the direction opposite to the electric field, in addition to the drift motion. This additional minute motion causes x_{1t} to be replaced by $x_{1t} - \delta_t$, where δ_t stands for the addition displacement of the electron cloud towards the collecting electrode at time t. Then the modified form of Eq. (8), taking the longitudinal diffusion of electrons into consideration, is given by

$$E_t = E\left(1-\frac{x_{1t}}{w}\right)+\frac{\delta_t}{w}E \qquad (16)$$

If one millimeter be the length of longitudinal diffusion experienced by electrons in traversing the distance w, the length of diffusion corresponding to the distance $w - x_{1t}$ will be given by $\delta_t = (w - x_{1t})/w$ mm. Since x_{1t}=0.7w, one gets δ_t =0.3mm. From Eq. (17) it is found that the error in the value of E, yielded by Eq. (8), caused by the longitudinal diffusion of electrons is only 0.25% of E and does not depend on the type of heavy ions. It may also be shown that the values of r are not affected by the longitudinal diffusion of electrons.

VI. Discussion

The effects of electron diffusion and ion motion do not effectively interfere in the proportionality between E_t and E, which may be transparent if Eqs. (16) and (17) are combined and written in the following form:

$$E_t = E\left(1-\frac{x_{1t}}{w}\right)+\left(1-\frac{x_{1t}}{w}\right)\left(\frac{E_{err(ion)}}{E}\right)E+\frac{\delta_t}{w}E$$

Here **$(E_{err(ion)}/E)$** is the only factor that varies with E. But the variation as shown in Fig. 4 is confined to a very small range of span less than 0.001. So this factor also may be taken to be invariant. Thus E_t remains almost proportional to **E**. This proportionality does not depend on the angle of incidence and the type of the heavy ion; hence it gives a scope to use a simple PMPPGIC, without Frisch grid, for estimating the energy of heavy ions.

In an ionization chamber which is operated at a pressure less than one atmosphere and under a suitable electric field [10], normally encountered in pulse mode gas ionization chambers, the probability of recombination between electrons and positive ions is extremely small and the electron drift velocity is negligibly

influenced by the positive ions. Because of the low recombination probability the effect of pulse height defect, caused by recombination, is not expected to be much significant. Hence it may be expected that this proportionality is applicable to a wide range of Z-values.

Eq. (11) can't be used for Z-identification of heavy ions unless the ionization tracks remain almost straight. So, this method of identification may not work in light ions (Z=1, 2) or very light heavy ions because of the large probability of range scattering. A study of the ion trajectories (in P-10 gas at pressure 600 torr), constructed with the help of SRIM 2008 calculations, yields that the possibility of range scattering tends to be insignificant from Z=7 onwards.

Eq. (11) remains valid irrespective of whether the heavy ion shows any deviation from its straight track. Because R_c gives the centroid of all the ions or electrons generated by the ionizing heavy ion. But, this equation cannot be used for the identification of the heavy ion if the track of ionization does not remain almost straight. Since in the case of heavy ions almost all of the tracks are supposed to be straight (unlike the light ions), the angle of incidence has been taken to be the same as the angle that R_c makes with the x-axis.

At a given initial energy the pattern of the distribution of the generated ion-electron pairs along the track of ionization depends on the identity of the heavy ion. The position of the centroid of the electrons or ions generated along the track of ionization depends obviously on the distribution pattern. The Bragg peak region, which is a part of the ionization track, contributes largely towards forming the pattern of the distribution. So the Bragg peak region of the track contributes towards setting the position of the centroid.

The Bragg peak occurs immediately before the moment at which the ion comes to rest. Because of very low speed at the Bragg peak region it may be possible that the heavy ion gets deviated from its straight track just at the end of its path. Also, because of very low speed the length of the deviated portion of the ion track is supposed to be very much small compared to the rest straight portion of the ion track. The heavy ion trajectories plotted using SRIM calculations depict the smallness in length of the deviated portion, if occurs. And this smallness causes the position of the centroid of the ions or electrons, generated along the deviated portion only, to remain very much closed to the straight portion of track. As a result the position of the centroid of all the electrons or ions generated along the whole ionization track either remains almost unchanged relative to - or experiences an extremely small shift from - the centroid of an identical ionization track that has experienced no deviation at the end. So the values of the projected R_c are expected to be confined to the spans estimated in Fig. 3.

VII. Conclusion

We shall not compare this technique of 'Z-identification of heavy ions' proposed in this theoretical work with alternative concepts. Instead, we may say that it is a low cost and simple technique and may be applicable to a wide range of Z-values, expectedly from Z=7 onwards.

References

[1] B. B. Rossi, et al., National Nuclear Energy Series, div. V.Vol.2, McGraw-Hill Book Company, Inc. New York, 1949.
[2] S. S. Kapoor, et al., in: Nuclear Radiation Detectors, New Age International (P) Limited, Publishers, 2001 chapter- III.
[3] O. Bunemann, et al., Can. J. Res., A27, 191 (1949).
[4] Rathin Saha, Nucl. Instr. and Meth A 620 (2010) 314.
[5] W. J. Price, Nuclear Radiation Detection, 2nd ed., Mc Grew-Hill Book Company, New York, 1964 pp.103.
[6] L. Bardelli, et al., Nucl. Instr. and Meth. A 491 (2002) 244.
[7] C. R. Gruhn, "Bragg curve spectroscopy" LBNL Paper LBL-12678, INS International Conference on Radiation Detectors, Tokyo, Japan, March 23-28, 1981.
[8] J. M. Asselineau et al., Nucl. Instr. and Meth. 204 (1982), 109-115
[9] G. F. Knoll, Radiation Detection and Measurement, 3rd ed., John Wiley and Sons, Inc., New York, 2000 chapter 5.
[10] H. W. Fulbright, Nucl. Instr. and Meth. 162(1979)21.